Pergamon

Int. J. Solids Structures Vol. 31, No. 12/13, pp. 1829–1846, 1994
Elsevier Science Ltd
Printed in Great Britain
0020-7683/94 $7.00 + .00

0020-7683(93)E0023-B

SOLIDIFICATION PROBLEMS BY THE BOUNDARY ELEMENT METHOD

NICHOLAS ZABARAS
Sibley School of Mechanical and Aerospace Engineering, Cornell University, Ithaca, NY 14853, U.S.A.

and

SUBRATA MUKHERJEE
Department of Theoretical and Applied Mechanics, Cornell University, Ithaca, NY 14853, U.S.A.

Abstract—This paper elaborates on the analysis and design of the solidification of pure metals. In the first part of this paper, a direct analysis is presented for the motion of the solid–liquid freezing interface and the time-dependent temperature field. An iterative implicit algorithm has been developed for this purpose using the boundary element method (BEM) with time dependent Green's functions and convolution integrals. Emphasis is placed on two-dimensional examples. The second part of this paper provides a methodology for the solution of an inverse design Stefan problem. A method for controlling the fluxes at the freezing front and its velocity is demonstrated. The BEM in conjunction with a sequential least squares technique are used to solve this ill-posed problem that has important technological applications. The accuracy of the method is illustrated through one-dimensional numerical examples.

1. INTRODUCTION

Problems of solidification of pure substances share the characteristic of an isothermal moving interface (freezing front). The freezing front motion and fluxes must be calculated as part of the solution of the phase change boundary value problem. Heat conduction is assumed in both solid and liquid phases and all thermal properties are considered temperature independent.

The flux discontinuity at any point of the interface is related to its normal velocity by the equation balancing the rate of heat flow with the energy rate required to create a fresh amount of solid per unit time (Stefan condition).

A solidification problem is considered direct when the temperature or the flux on the fixed boundary of a solidifying body, with given material properties, is prescribed.

There is an extensive literature on the above and related "Stefan" problems. The methods used to solve these problems can be categorized (Crank, 1984) into analytical, front-tracking, front-fixing and fixed-domain methods. The existing analytical solutions are primarily for one-dimensional problems (Crank, 1984) and two-dimensional wedge-shaped spaces (Budhia and Kreith, 1973; Rathjen and Jiji, 1971).

Front-tracking methods involve finite differences or finite elements on a fixed grid (Lazaridis, 1969; Rao and Sastri, 1984), or on a variable space grid (Murray and Landis, 1959) or the use of adaptive meshes (Bonnerot and Janet, 1977; Lynch, 1982; Albert and O'Neill, 1986; Zabaras and Ruan, 1990). An alternative formulation includes front-fixing methods (Crank and Gupta, 1975) where the moving front is fixed by a suitable choice of space coordinates. In the fixed-domain methods the problem is formulated in such a way that the interface condition becomes implicit in a new form of the equations, which applies over the whole of a fixed domain (Ralph and Bathe, 1982; Hsiao, 1985; Voller and Cross, 1981; Roose and Storrer, 1984).

Integral formulations for one-dimensional problems have been applied extensively in the past (Chuang and Szekely, 1972; Banerjee and Shaw, 1982; Heinlein *et al.*, 1986; O'Neill, 1983; Sadegh *et al.*, 1985). O'Neill (1983) gave a general integral formulation for quasi-static phase change problems, while Zabaras and Mukherjee (1987) extended this work to transient problems. Similar work has also been reported by Sadegh *et al.* (1985).

Hong *et al.* (1984) have solved two-dimensional solidification problems by updating the position of the interface at each time step while keeping the interface location fixed during the calculation of the temperature field at each time step.

This first part of this paper is concerned with a BEM formulation of two-dimensional direct solidification problems. The general integral equations are presented together with their numerical implementation. Special emphasis is given on key issues such as the accurate calculation of singular integrals, the iterative technique and the calculation of the interface motion. Numerical results for some sample two-dimensional solidification problems are presented and discussed. The detailed analysis is presented in an earlier publication by the authors (Zabaras and Mukherjee, 1987).

Design Stefan problems, where the temperature, fluxes and velocity are prescribed on the freezing front, while the temperature and the flux on the fixed boundary of the domain of interest are unknown and must be determined by the analysis, are also discussed in this paper. They were first introduced in one dimension by Zabaras *et al.* (1988) who extended Beck's (Beck *et al.*, 1985) sensitivity analysis to problems with phase changes using a BEM analysis. By controlling the freezing interface fluxes and velocities during solidification the cast structure can be controlled and made more uniform (Zabaras *et al.*, 1988; Flemings, 1974). Further discussion and finite element results of such inverse design Stefan problems are given in recent publications by Zabaras and co-workers (Zabaras and Ruan, 1989; Zabaras, 1990; Ruan and Zabaras, 1991; Zabaras *et al.*, 1992). Here, our work reported in Zabaras *et al.* (1988) is extended to two-dimensional problems. Smoothing in time and space is introduced in the sense used by Zabaras *et al.* (1992). The BEM analysis allows easy and accurate calculation of the sensitivity coefficients and provides certain other advantages by permitting direct calculation of the surface fluxes. Typical one-dimensional results are reported and discussed at the end of this paper.

2. DIRECT ANALYSIS OF SOLIDIFICATION

2.1. *Governing differential equations*

A liquid at an initially uniform temperature T_i (equal to or above the melting point T_m) is assumed to occupy a region with a fixed boundary ∂B_0. At time $t > 0$, the boundary ∂B_0 is cooled to a temperature lower than the melting temperature T_m. Solidification starts all around ∂B_0 and proceeds inwards. The interface at some time t is denoted by ∂B_I (Fig. 1).

The governing differential equations, in the absence of heat sources and with constant material parameter, are (Crank, 1984):

$$\frac{\partial T_s}{\partial t}(\mathbf{x}, t) = k_s \nabla^2 T_s(\mathbf{x}, t) \quad \mathbf{x} \in B_S, \tag{1}$$

$$\frac{\partial T_l}{\partial t}(\mathbf{x}, t) = k_l \nabla^2 T_l(\mathbf{x}, t) \quad \mathbf{x} \in B_L, \tag{2}$$

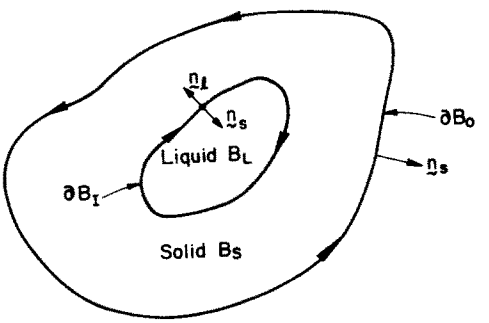

Fig. 1. Geometry of the solidification problem [from Zabaras and Mukherjee (1987)].

where for example, $T_s(\mathbf{x}, t)$ is the temperature at the point $\mathbf{x} \in B_s$ at time t and the rest of the notation is clear from Fig. 1.

The thermal diffusivity k_s of the solid phase is equal to $K_s/\rho_s c_s$ in terms of its conductivity K_s, densitiy ρ_s and specific heat c_s, respectively. Similar notation is used for k_l. The boundary, initial and freezing interface conditions are given as:

$$T(\mathbf{x}, t) = T_0(\mathbf{x}, t) \quad \mathbf{x} \in \partial B_{0_1}, \tag{3a}$$

$$K_s \frac{\partial T}{\partial n} \equiv q(\mathbf{x}, t) = q_0(\mathbf{x}, t) \quad \mathbf{x} \in \partial B_{0_2}, \tag{3b}$$

$$T(\mathbf{x}, t) = T_m \quad \mathbf{x} \in \partial B_I, \tag{3c}$$

$$K_s \frac{\partial T_s}{\partial n_s} - K_l \frac{\partial T_l}{\partial n_s} = \rho_s L \frac{\partial V_n}{\partial t} \quad \mathbf{x} \in \partial B_I, \tag{3d}$$

$$B_S = 0 \quad \text{at} \quad t = 0, \tag{3e}$$

$$T(\mathbf{x}, 0) \equiv T_i = \text{const} \quad \mathbf{x} \in B_L(0), \tag{3f}$$

where T_0 is a prescribed temperature history on the part ∂B_{0_1} of ∂B_0 and q_0 is the prescribed flux on the remaining part ∂B_{0_2} of ∂B_0, T_m is the melting point of the solid and L the latent heat of fusion. Further, V_n is the normal velocity of the solidification front at a point on ∂B_I.

To simplify the involved calculations we assume that T_i is constant throughout $B_L(0)$. With new simplified notations for fluxes, one can write the freezing interface normal velocity in the form

$$V_n = \frac{1}{\rho_s L} q_{ms} - \frac{1}{\rho_s L} q_{ml}, \tag{4}$$

where

$$q_{ms} = K_s \frac{\partial T_s}{\partial n_s} \quad \text{and} \quad q_{ml} = K_l \frac{\partial T_l}{\partial n_s} \quad \text{for} \quad \mathbf{x} \in \partial B_i.$$

A direct solidification problem is defined as one of solving eqns (1)–(4) for the interface normal velocity V_n, and the temperature field. This can be achieved by solving the integral equations as presented next.

2.2. *Integral formulation*

One can write the following integral equations (Zabaras and Mukherjee, 1987). For the solid phase, with $P \in \partial B_s \equiv \partial B_0 \cup \partial B_I$:

$$\begin{aligned} c(P)T(P, t) = &\int_0^t \mathrm{d}t_0 \int_{\partial B_0} \left[G_s(P, t; Q, t_0) q_0(Q, t_0) - k_s \frac{\partial G_s}{\partial n_s}(P, t; Q, t_0) T_0(Q, t_0)\right] \mathrm{d}s_Q \\ &+ \int_0^t \mathrm{d}t_0 \int_{\partial B_I} \left[G_s(P, t; Q, t_0) q_{ms}(Q, t_0) - k_s \frac{\partial G_s}{\partial n_s}(P, t; Q, t_0) T_m \right. \\ &\left. + G_s(P, t; Q, t_0) T_m V_n(Q, t_0)\right] \mathrm{d}S_Q \end{aligned} \tag{5}$$

with the temperature T on the left-hand side of the above equation being equal to T_m and T_0, respectively, for the cases $P \in \partial B_I$ and $P \in \partial B_0$. These equations are called (5a) and (5b), respectively, for ease of reference.

For the liquid phase, with $P \in \partial B_I$

$$c(P)(T_m - T_i) = \int_0^t \mathrm{d}t_0 \int_{\partial B_1} [G_l(P,t;Q,t_0)(-q_{ml}(Q,t_0)) - k_l \frac{\partial G_l}{\partial n_l}(P,t;Q,t_0)(T_m - T_i) + G_l(P,t;Q,t_0)(T_m - T_i)(-V_n(Q,t_0))]\,\mathrm{d}S_Q \quad (6)$$

with the Green's functions G_s and G_l defined as

$$G(p,t;q,t_0) = \frac{\exp\left[-\dfrac{r^2}{4k(t-t_0)}\right]}{[4\pi k(t-t_0)]^{m/2}}, \quad (7)$$

where m is the dimension of the problem and $c(P)$ in eqns (5) and (6) is specified as in Zabaras and Mukherjee (1987).

A major simplification arises in eqn (6) if $T_i = T_m$.

2.3. *Numerical implementation*

The solution strategy consists of the use of suitable shape functions, in space as well as in time, for the unknowns of the problem, and marching forward in time. The solid–liquid interface, of course, is part of the solution and must be updated continuously in time. Convolution type integrals must be calculated over a variable domain all the way from the initial zero time.

The boundaries ∂B_0 and ∂B_1 are divided into N_1 and N_2 (at time zero) linear straight segments. The freezing interface mesh is considered, in general, a function of time. This is in order to account for the movement of the freezing front. Omitting indications of source and field points, the discretized forms of eqns (5a), (5b) and (6) are:

For the solid phase, with $P \in \partial B_1$

$$c(P)T_m(t_F) = \sum_{f=1}^{F} \int_{t_{f-1}}^{t_f} \mathrm{d}t_0 \sum_{k=1}^{N_1} \int_{\partial B_{0_k}} \left[G_s q_0 - k_s \frac{\partial G_s}{\partial n_s} T_0\right]\mathrm{d}S_Q + \int_{f=1}^{F} \int_{t_{f-1}}^{t_f} \mathrm{d}t_0 \sum_{k=1}^{N_2(t_0)} \int_{\partial B_{1_k}} \left[G_s(q_{ms} + T_m V_n) - k_s \frac{\partial G_s}{\partial n_s} T_m\right]\mathrm{d}S_Q \quad (8)$$

and, with $P \in \partial B_0$

$$c(P)T_0(P,t_F) = \sum_{f=1}^{F} \int_{t_{f-1}}^{t_f} \mathrm{d}t_0 \sum_{k=1}^{N_1} \int_{\partial B_{0_k}} \left[G_s q_0 - k_s \frac{\partial G_s}{\partial n_s} T_0\right]\mathrm{d}S_Q + \sum_{f=1}^{F} \int_{t_{f-1}}^{t_f} \mathrm{d}t_0 \sum_{k=1}^{N_2(t_0)} \int_{\partial B_{1_k}} \left[G_s(q_{ms} + T_m V_n) - k_s \frac{\partial G_s}{\partial n_s} T_m\right]\mathrm{d}S_Q. \quad (9)$$

For the liquid phase, with $P \in \partial B_1$

$$c(P)(T_m(t_F) - T_i) = \sum_{f=1}^{F} \int_{t_{f-1}}^{t_f} \mathrm{d}t_0 \sum_{k=1}^{N_2(t_0)} \int_{\partial B_{1_k}} \left[G_l(-q_{ml} - (T_m - T_i)V_n) - k_l \frac{\partial G_l}{\partial n_l}(T_m - T_i)\right]\mathrm{d}S_Q. \quad (10)$$

Note that the interface velocity and position enter the above equations in an explicit as well as in an implicit and nonlinear manner through the Green's functions.

Linear shape functions in space and in time are chosen here. Specifically, for the time step (t_{f-1}, t_f), and for a straight boundary element on ∂B_1 with nodes 1 and 2 denoting the start and end of the element, the flux q_{ms}, for example, can be written as

$$q_{ms} = \phi_1\psi_1 q_{ms_1}^{f-1} + \phi_2\psi_1 q_{ms_2}^{f-1} + \phi_1\psi_2 q_{ms_1}^{f} + \phi_2\psi_2 q_{ms_2}^{f}, \tag{11}$$

where the spatial and time shape functions ϕ_i and ψ_i are given as

$$\phi_1 = 1 - s/\Delta s, \quad \phi_2 = s/\Delta s, \tag{12}$$

$$\psi_1 = (t_f - t_0)/\Delta t_f, \quad \psi_2 = (t_0 - t_{f-1})/\Delta t_f, \tag{13}$$

with $\Delta t_f = t_f - t_{f-1}$ and $q_{ms_i}^f$ denoting the nodal flux at node i at time t_f. The distance s is measured along the element of length $\Delta s(t)$, starting at node 1. Expressions similar to (12) are also valid for q_{ml}, V_n and q_0.

The integrals which appear in eqns (8)–(10) have one of the following forms:

$$I_{i1} = k\int_{t_{f-1}}^{t_f} \mathrm{d}t_0 \int_{\partial B_k} \psi_i \frac{\partial G}{\partial n}\,\mathrm{d}s, \tag{14a}$$

$$I_{i2} = k\int_{t_{f-1}}^{t_f} \mathrm{d}t_0 \int_{\partial B_k} \frac{s}{\Delta s}\psi_i \frac{\partial G}{\partial n}\,\mathrm{d}s, \tag{14b}$$

$$I_{i3} = \int_{t_{f-1}}^{t_f} \mathrm{d}t_0 \int_{\partial B_k} \psi_i G\,\mathrm{d}s, \tag{14c}$$

$$I_{i4} = \int_{t_{f-1}}^{t_f} \mathrm{d}t_0 \int_{\partial B_k} \frac{s}{\Delta s}\psi_i G\,\mathrm{d}s, \tag{14d}$$

for $i = 1, 2$ and ∂B_k an element on the stationary boundary ∂B_0 or on the moving interface ∂B_1. The source point of reference in the above integrals can lie on ∂B_0 or ∂B_1.

2.4. *Evaluation of integrals*

(a) Integration over ∂B_0 with source point on ∂B_0. This case includes integrals similar to those for non-phase change heat condition problems [see Brebbia *et al.* (1984)].

(b) Integration on ∂B_0 with source point on ∂B_1. With estimation of the position of the source point a Gaussian integration in space and in time can be effective (no singular integrals appear in this category). The interface position at time t_F can be estimated, by assuming that the interface moves during the interval (t_{F-1}, t_F) with the velocity it has at time t_{F-1}.

(c) Integration over ∂B_1 with source point on ∂B_0

(i) case $t_f = t_F$
Using an estimate of the position of the interface during the interval (t_{F-1}, t_F), simple Gaussian integration can be effective.

(ii) case $t_f \neq t_F$
Considering that the interface is moving on the interval (t_{f-1}, t_f) with the constant known velocity $(V_f + V_{f-1})/2$, Gaussian integration can be used, where V_f and V_{f-1} are the velocities at the end and beginning of the time interval.

(d) Integration over ∂B_1 with source point on ∂B_1.

(i) case $t_f \neq t_F$
This case is very similar to the cases (b) and (c) above

(ii) $t_f = t_F$
If the source point $P \notin \partial B_{1_k}$ similar ideas as above can be applied. The singular

case $P \in \partial B_{l_k}$ requires special care. Splitting, for example (14d), into two parts I'_{i3} and I''_{i3}

$$I_{i3} = \int_{t_{F-1}}^{t_F^*} \mathrm{d}t_0 \int_{\partial B_{l_k}} \psi_i G \, \mathrm{d}S + \int_{t_F^*}^{t_F} \mathrm{d}t_0 \int_{\partial B_{l_k}} \psi_i G \, \mathrm{d}S,$$

where

$$t_F^* = t_{F-1} + \tfrac{3}{4}(t_F - t_{F-1})$$

the first integral I'_{i3} is nonsingular and can be evaluated as before. The singular integral I''_{i3} is obtained as follows. Since the interval $t_F - t_F^*$ is small, it is assumed that the order of the spatial and time integral can be reversed in this case even though the interface element moves a little during this time interval. This assumption permits I''_{i3} to be evaluated analytically as is done for the integrals in case (a) above. The shape functions in I''_{i3} are defined over the entire interval t_{F-1}, t_F. The final expressions for these integrals are given in Zabaras and Mukherjee (1987).

2.5. *Modeling of corners*

Single corner nodes on the interface ∂B_I. A length weighted average normal $\mathbf{n}$ at the corner node i is defined as

$$\mathbf{n} = (l_{i-1}\mathbf{n}_{i-1} + l_i \mathbf{n}_i)/(l_{i-1} + l_i) \tag{15}$$

in terms of the lengths l_{i-1} and l_i and unit normals $\mathbf{n}_{i-1}$ and $\mathbf{n}_i$ of contiguous elements. The normal velocity V_n at node i is now assigned along the unit vector $\mathbf{n}/|\mathbf{n}|$.

Physical corners on the freezing interface are modelled by double nodes. Let $V_n(i)$ and $V_n(i+1)$ be the normal velocities at the (physically same) nodes i and $i+1$. To avoid singular matrices, we assume that the physical corner has a unique velocity of magnitude V_n in the average normal direction $\mathbf{n}$ defined by eqn (15) with l_i and $\mathbf{n}_i$ replaced by l_{i+1} and $\mathbf{n}_{i+1}$ respectively.

An independent relation between $V_{n(i)}$ and $V_{n(i+1)}$ results as

$$V_{n(i)}(\mathbf{n} \cdot \mathbf{n}_{i+1}) - V_{n(i+1)}(\mathbf{n} \cdot \mathbf{n}_{i-1}) = 0. \tag{16}$$

The tangential motion of the freezing interface modes does not come into the physics of the problem. However, it has to be specified artificially by the analyst so that the proper mesh is always preserved on ∂B_I. Further discussion of the importance of the tangential motion of interface nodes is given in Zabaras and Ruan (1990).

Double nodes are also used at points on ∂B_0 in order to allow for flux discontinuities across geometric corners. An interesting situation arises at a physical corner on ∂B_0 if the temperature T is prescribed on both elements meeting there. Again, a singular matrix can be avoided in this situation by including an extra equation. The unknown flux at one of the double nodes is replaced by the flux obtained by backward differences from the prescribed temperatures on contiguous elements at these nodes.

2.6. *Matrix formulation*

Let us consider the case when T_0 is prescribed all over ∂B_0. Equations (4) and (8)–(9) contain the unknown nodal boundary vectors $\mathbf{q}_{ms}^F$, $\mathbf{q}_{ml}^F$ and $\mathbf{q}_0^F$ at time t_F. In matrix form we can write them as:

$$\begin{bmatrix} [A]_\alpha & [A]_\beta & [\Delta] \\ [B]_\alpha & [B]_\beta & [E] \\ [\Gamma]_\gamma & [\Gamma]_\delta & [\phi] \end{bmatrix} \begin{bmatrix} \mathbf{q}_{ms}^F \\ \mathbf{q}_{ml}^F \\ \mathbf{q}_0^F \end{bmatrix} = \begin{bmatrix} \varepsilon \\ \zeta \\ \eta \end{bmatrix}, \tag{17}$$

where

$$\alpha = 1 + T_m/\rho L, \tag{18a}$$

$$\beta = -T_m/pL, \tag{18b}$$

$$\gamma = -(T_m - T_i)/\rho L, \tag{18c}$$

$$\delta = -1 + (T_m - T_i)/\rho L \tag{18d}$$

and $[\phi]$ denotes the zero matrix. The matrices $[A]$, $[B]$, $[\Gamma]$, $[\Delta]$ and $[E]$ contain calculations over the last time step (t_{F-1} to t_F). The vectors on the right side of (17) are known from previous calculations (time zero to t_{F-1}) and the applied boundary conditions, and they are *not* given explicitly here.

For the case $T_m = T_i$ a reduced form of eqn (17) (with $\mathbf{q}_{ml} = 0$) has been used. For the superheated case ($T_i > T_m$) eqn (17) has been combined with the following equation:

$$\frac{1}{\rho L}(\mathbf{q}_{ms}^F - \mathbf{q}_{ml}^F) = \mathbf{V}_{pr}, \tag{19}$$

where $\mathbf{V}_{pr}$ is the predicted velocity vector in the time interval t_{F-1} to t_F.

Equations (18) and (19) have been solved in a least squares sense for the flux vectors $\mathbf{q}_{ms}$, $\mathbf{q}_{ml}$ and $\mathbf{q}_0$. Equation (19) is introduced in order to avoid numerical divergence which appears at early times, when $\partial B_0 = \partial B_{0_2}$ and when eqn (17) is used alone. It is obvious that a proper scaling of eqns (17) and (19) has to be used before their final solution.

A simple iterative procedure is adopted here. Before updating the geometry and continuation to the next time step, one must check if the nodal positions on ∂B_1 at time t_F, predicted at the end of a successful iteration, are such that numerical instabilities could appear at the next time step t_F to t_{F+1}. These instabilities usually occur when the freezing interface nodes come very close to each other. If this is the case, then remeshing must be performed by node removal or node rearrangement (i.e. by introducing nodal motion tangential to the interface).

The advantage of this BEM formulation with respect to the so-called "domain methods" and other front tracking techniques is that for the calculation of the temperature at points internal to the domain one does not have to calculate all the internal temperatures over the entire domain. The equation corresponding to internal temperature calculation is not given here, but it has a form similar to that of the boundary equations given earlier. Two disadvantages are also present in the BEM analysis. At first, like in other front tracking techniques (Zabaras and Ruan, 1990), one must assume at time zero the existence of some solid (Zabaras and Mukherjee, 1987). The second major disadvantage is that the fluxes q_{ms} and q_{ml} appear separately in the analysis and not in the combined form which yields the normal interface velocity [see eqn (4)]. As a result, the direct calculation of both interface fluxes leads to progressively incorrect front motion which can eventually violate global energy conservation. For a weak form of the Stefan condition, an energy conserving scheme and more references on the subject see Zabaras and Ruan (1990).

3. AN INVERSE/DESIGN SOLIDIFICATION PROBLEM

3.1. *The problem*

Of concern here is an inverse-design solidification problem that is defined as follows: "Given the thermal properties of the solid and liquid phases and the melting temperature,

calculate the boundary flux/temperature on ∂B_0 that achieves a desired freezing front motion."

For solidification in a one-dimensional region $0 \leqslant x \leqslant l$, one must specify the interface fluxes $q_{ms}(t)$ and $q_{ml}(t)$ instead of specifying only the interface motion $V(t)$. In this case, Zabaras *et al.* (1988) have shown that two uncoupled inverse problems arise: one in the solid and another in the liquid phase. They derived an unstable analytical solution in the form of an infinite series involving the prescribed interface flux and velocity and their time derivatives.

The importance of the above and related design solidification problems lies in the fact that the quality of the solidifying crystals is directly related to the freezing interface fluxes and velocity rather than the applied cooling boundary conditions on $\partial\Omega_0$. These problems are ill-posed in the sense that their solution may not be unique and stable to small changes in the desired interface motion. Here a general methodology will be presented for two-dimensional problems and some one-dimensional examples will be discussed.

3.2. *Future information and spatial regularization methods*

The boundary element analysis prescribed earlier is a convenient tool for the analysis of the above design problem since the freezing interface position/motion is known *a priori*. Indeed, let us consider a boundary element discretization of $\partial\Omega_0$ and $\partial\Omega_1$ and a time stepping process. The main unknowns of the design problem are considered to be the nodal fluxes (or temperatures) all over $\partial\Omega_0$. Let $\mathbf{q}_0^F$ denote the boundary nodal unknown fluxes on ∂B_0 at $t = t_F$, i.e.

$$\mathbf{q}_0^F = \{q_{01}^F, q_{02}^F, \ldots, q_{0i}^F, \ldots, q_{0N_1}^F\}^{\mathrm{T}}, \tag{20}$$

where N_1 is the number of variables to be estimated, and q_{0i}^F are the boundary heat fluxes at the ith boundary nodes and at time t_F. The given interface motion/position is treated as a boundary condition on ∂B_1. Then, one can consider that the temperature field at any point inside the domain is a function of $\mathbf{q}_0^F$ (through the solution of a direct boundary value problem). Assume that the temperature distribution at time t_{F-1} is known and that $\mathbf{q}_{0*}^F$ is an estimate of the vector of boundary nodal fluxes. Let the times t_{F+i-1}, $i = 1, 2, \ldots, r$, be future times with $r-1$ denoting the number of future time steps and N_2 be the number of nodes on ∂B_1. Then, following Beck *et al.* (1985), the vector $\mathbf{q}_0^{F+i-1}$ is temporally constrained to be given as $\mathbf{q}_0^{F+i-1} = \mathbf{q}_{0*}^F$, $i = 1, 2, \ldots, r$. The temperatures at the N_2 nodal points in the solid/liquid interface at time t_{F+i-1} can be approximated using the following truncated Taylor series expansion:

$$T_k^{F+i-1} = \overset{*}{T}{}_k^{F+i-1} + \frac{\partial T_k^{F+i-1}}{\partial \mathbf{q}_0^F}(\mathbf{q}_0^F - \mathbf{q}_{0*}^F), \quad k = 1, 2, \ldots, N_2, \quad i = 1, 2, \ldots, r. \tag{21}$$

Equation (21) can be written in a compact form as

$$\mathbf{T} = \overset{*}{\mathbf{T}} + \mathbf{S}(\mathbf{q}_0^F - \mathbf{q}_{0*}^F), \tag{22}$$

where

$$\mathbf{T} = (\mathbf{T}_1, \mathbf{T}_2, \ldots, \mathbf{T}_i, \ldots, \mathbf{T}_r)^{\mathrm{T}} \quad \text{with} \quad \mathbf{T}_i = (T_1^{F+i-1}, T_2^{F+i-1}, \ldots, T_k^{F+i-1}, \ldots, T_{N_2}^{F+i-1})^{\mathrm{T}} \tag{23}$$

and the sensitivity matrix S is defined as

$$\mathbf{S} = (\mathbf{S}_1, \mathbf{S}_2, \ldots, \mathbf{S}_i, \ldots, \mathbf{S}_r)^{\mathrm{T}} \quad \text{where} \quad \mathbf{S}_i = (S_1^{F+i-1}, S_2^{F+i-1}, \ldots, S_k^{F+i-1}, \ldots, S_{N_2}^{F+i-1})^{\mathrm{T}} \tag{24}$$

with

$$\mathbf{S}_k^{F+i-1} = \frac{\partial T_k^{F+i-1}}{\partial \mathbf{q}_0^F}. \tag{25}$$

The vector $\overset{*}{\mathbf{T}}$ has a form similar to the vector $\mathbf{T}$ and is calculated through a direct problem, using $\mathbf{q}_{0^*}^F$ and the known freezing front motion. More details on this will be given later.

The goal is to calculate the optimum value of the vector $\mathbf{q}_0^F$ such that the error between the approximated temperatures T_k^{F+i-1} and the given interface temperature (T_m) is minimum, i.e.

$$\min_{\mathbf{q}_0^F} \{(\mathbf{Y}-\mathbf{T})^{\mathrm{T}}\mathbf{W}(\mathbf{Y}-\mathbf{T}) + \alpha_0(\mathbf{q}_0^F)^{\mathrm{T}}\mathbf{W}_0\mathbf{q}_0^F + \alpha_1(\mathbf{H}\mathbf{q}_0^F)^{\mathrm{T}}\mathbf{W}_1(\mathbf{H}\mathbf{q}_0^F)\}, \tag{26}$$

where α_0 and α_1 are regularization parameters with $\alpha_0 > 0$, $\alpha_1 > 0$, $\mathbf{W}$, $\mathbf{W}_0$ and $\mathbf{W}_1$ are optimization weighting matrices and $\mathbf{H}$ is the first order spatial regularization coefficient matrix. These matrices are discussed in detail in Zabaras *et al.* (1992). The vector $\mathbf{Y}$ is defined as

$$\mathbf{Y} = (\mathbf{Y}_1, \mathbf{Y}_2, \ldots, \mathbf{Y}_i, \ldots, \mathbf{Y}_r)^{\mathrm{T}} \quad \text{where} \quad \mathbf{Y}_i = (T_m, T_m, \ldots, T_m, \ldots, T_m). \tag{27}$$

The second term in eqn (26) has been added to keep the estimated boundary fluxes at finite values, and the last term is necessary to avoid large flux variation between adjacent nodal points (Tikhonov and Arsenin, 1977). Performing the minimization and after some manipulation,

$$\mathbf{q}_0^F = (\mathbf{S}^{\mathrm{T}}\mathbf{W}\mathbf{S} + \alpha_0\mathbf{W}_0 + \alpha_1\mathbf{H}^{\mathrm{T}}\mathbf{W}_1\mathbf{H})^{-1}[\mathbf{S}^{\mathrm{T}}\mathbf{W}(\mathbf{Y}-\overset{*}{\mathbf{T}}) + \mathbf{S}^{\mathrm{T}}\mathbf{W}\mathbf{S}\mathbf{q}_{0^*}^F]. \tag{28}$$

A discussion on the selection of the regularization parameters is given in Zabaras *et al.* (1992). Using eqn (28), the boundary nodal unknowns can be found. The temperature field can then be obtained by solving a direct boundary value problem. An iterative procedure must be performed due to the nonlinearity of the problem. For a related BEM analysis of an inverse elasticity problem see Zabaras *et al.* (1989).

Calculation of $\overset{*}{\mathbf{T}}$. To evaluate $\overset{*}{\mathbf{T}}$ one must solve a direct problem with prescribed flux $\mathbf{q}_{0^*}^F$ and ∂B_0 and known interface motion on ∂B_1. This is a slightly different direct problem from the one presented in the first part of this paper.

The integral eqns (4) and (8)–(10) provide (N_1+3N_2) equations that can be solved for the (N_1+3N_2) unknowns which include $\mathbf{T}_0^F(N_1)$, $\mathbf{q}_{ms}^F(N_2)$, $\mathbf{q}_{ml}^F(N_2)$ and $\overset{*}{\mathbf{T}}(N_2)$. It must be emphasized again that it is the interface velocity [i.e. from eqn (4) the interface flux discontinuity] rather than the individual interface fluxes, $\mathbf{q}_{ms}$ and $\mathbf{q}_{ml}$ that are required in solving this direct problem.

3.3. *Calculation of the sensitivity coefficients*

An easy and rather obvious way to calculate sensitivity coefficients is by finite differences approximations. For example, one can write

$$\frac{\partial T_k^{F+i-1}}{\partial q_{0a}^F} \approx \frac{\overset{**}{T}{}_k^{F+i-1} - \overset{*}{T}{}_k^{F+i-1}}{\lambda q_{0a}^{*F}} \quad k = 1,2,\ldots,N_2;\ i = 1,2,\ldots,r;\ a = 1,2,\ldots,N_1, \tag{29}$$

where temperature $\overset{**}{\mathbf{T}}$ is calculated by solving the direct problem similar to $\overset{*}{\mathbf{T}}$ with the boundary condition $(1+\lambda)\mathbf{q}_0^F$, and $\lambda = 0.001$.

An alternative, direct and more accurate way of calculating these sensitivity coefficients using the BEM was presented by Zabaras *et al.* (1988). To demonstrate the calculation of the sensitivity coefficients at t_F, let us write eqns (8), (9), and (10) in a matrix form as follows [see Brebbia *et al.* (1984) for notation].

Equation (8) may be written as:

$$\mathbf{A}_F^F\mathbf{T}_0^F + \mathbf{AI}_F^F\mathbf{T}_m^F = \mathbf{B}_F^F\mathbf{q}_0^F + \mathbf{BI}_F^F\mathbf{q}_{ms}^F + \mathbf{A}_F^{F-1}\mathbf{T}_0^{F-1} + \mathbf{AI}_F^{F-1}\mathbf{T}_m^{F-1} + \mathbf{B}_F^{F-1}\mathbf{q}_0^{F-1} + \mathbf{BI}_F^{F-1}\mathbf{q}_{ms}^{F-1} + \cdots, \tag{30}$$

where all matrices $\mathbf{A}_F^J$ and $\mathbf{B}_F^J$, $J = F,\ldots,1$ are of order $N_1 \times N_1$, and all matrices $\mathbf{AI}_F^J$ and $\mathbf{BI}_F^J$, $J = F,\ldots,1$ are of order $N_1 \times N_2$.

Similarly eqn (9) becomes

$$\mathbf{C}_F^F\mathbf{T}_0^F + \mathbf{CI}_F^F\mathbf{T}_m^F = \mathbf{D}_F^F\mathbf{q}_0^F + \mathbf{DI}_F^F\mathbf{q}_{ms}^F + \mathbf{C}_F^{F-1}\mathbf{T}_0^{F-1} + \mathbf{CI}_F^{F-1}\mathbf{T}_m^{F-1} + \mathbf{D}_F^{F-1}\mathbf{q}_0^{F-1} + \mathbf{DI}_F^{F-1}\mathbf{q}_{ms}^{F-1} + \cdots, \tag{31}$$

where all matrices $\mathbf{C}_F^J$ and $\mathbf{D}_F^J$, $J = F,\ldots,1$ are of order $N_1 \times N_1$, while $\mathbf{CI}_F^J$ and $\mathbf{DI}_F^J$ are of order $N_1 \times N_2$.

Finally, eqn (10) becomes

$$\mathbf{G}_F^F\mathbf{T}_m^F = \mathbf{E}_F^F\mathbf{q}_{ml}^F + \mathbf{G}_F^{F-1}\mathbf{T}_m^{F-1} + \mathbf{E}_F^{F-1}\mathbf{q}_{ml}^{F-1} + \cdots. \tag{32}$$

Subscripts in the above matrices denote current time of reference, while superscripts denote the time interval during which the integration is carried out. $\mathbf{T}_0^J$ denotes all nodal temperatures on ∂B_0 at time t_J, $\mathbf{q}_0^J$ all nodal fluxes at t_J and $\mathbf{q}_{ms}^J$ and $\mathbf{q}_{ml}^J$ the interface fluxes in the solid and liquid phases respectively. Finally, $\mathbf{T}_m^J$ are the calculated temperatures at the moving front. Note that the above matrices can be easily calculated in an explicit manner since the freezing front motion is *a priori* known. One-dimensional calculations can be found in Zabaras *et al.* (1988).

Let us assume that the interface velocity is given. We want to find the sensitivity of $\mathbf{T}_m^F$ with respect to $\mathbf{q}_0^F$, i.e. $\partial\mathbf{T}_m^F/\partial\mathbf{q}_0^F$.

Let us rewrite eqns (30)–(32) as follows:

$$\begin{bmatrix} \mathbf{A}_F^F & \mathbf{AI}_F^F & -\mathbf{BI}_F^F & 0 \\ \mathbf{C}_F^F & \mathbf{CI}_F^F & -\mathbf{DI}_F^F & 0 \\ 0 & \mathbf{G}_F^F & 0 & -\mathbf{E}_F^F \\ 0 & 0 & \mathbf{I} & -\mathbf{I} \end{bmatrix} \begin{Bmatrix} \mathbf{T}_0^F \\ \mathbf{T}_m^F \\ \mathbf{q}_{ms}^F \\ \mathbf{q}_{ml}^F \end{Bmatrix}$$

$$= \begin{bmatrix} \mathbf{B}_F^F & 0 \\ \mathbf{D}_F^F & 0 \\ 0 & 0 \\ 0 & \rho L\mathbf{I} \end{bmatrix} \begin{Bmatrix} \mathbf{q}_0^F \\ \mathbf{V}^F \end{Bmatrix} + \text{known terms from calculations at earlier times} \tag{33}$$

where $\mathbf{I}$ is a unit diagonal matrix of order $N_2 \times N_2$.

From eqn (33) it becomes obvious that the required sensitivity coefficients are given as

$$\begin{bmatrix} \partial \mathbf{T}_m^F \\ \overline{\partial \mathbf{q}_0^F} \end{bmatrix} = \begin{bmatrix} \mathbf{A}_F^F & \mathbf{AI}_F^F & -\mathbf{BI}_F^F & 0 \\ \mathbf{C}_F^F & \mathbf{CI}_F^F & -\mathbf{DI}_F^F & 0 \\ 0 & \mathbf{G}_F^F & 0 & -\mathbf{E}_F^F \\ 0 & 0 & \mathbf{I} & -\mathbf{I} \end{bmatrix}^{-1} \begin{bmatrix} \mathbf{B}_F^F & 0 \\ \mathbf{D}_F^F & 0 \\ 0 & 0 \\ 0 & \rho L \mathbf{I} \end{bmatrix} \begin{bmatrix} 0 \\ \vdots \\ 0 \\ 1 \\ 1 \\ \vdots \\ 1 \\ 0 \\ \vdots \\ 0 \end{bmatrix}, \tag{34}$$

where the unit elements in the vector on the right-hand side of the equation above start at the location (N_1+1) and end at the location (N_1+N_2). The matrix inversion indicated in eqn (34) must be performed analytically. This can be computationally inefficient, especially if (N_1+3N_2) is too large.

We have not yet investigated the merits of eqn (34) relative to those of eqns (29). Note that to evaluate $\partial \mathbf{T}_m^J / \partial \mathbf{q}_0^F$, $J = F+1, \ldots, F+r-1$, one should write equations similar to eqn (33) where the reference time is *not* t_F but t_{F+i-1}, $i = 2, \ldots, r$. In doing so, the boundary fluxes should be regularized in time such that

$$\mathbf{q}_0^{F+i-1} = \mathbf{q}_0^F, \quad i = 1, 2, \ldots, r.$$

Details and final expressions for one-dimensional problems can be found in Zabaras *et al.* (1988).

4. NUMERICAL EXAMPLES

4.1. *Dimensionless parameters*

For the problems to be considered the following dimensionless parameters have been used:

$$\mathbf{K}_s = 1, \quad \mathbf{K}_l = K_l/K_s, \quad \mathbf{c}_s = 1, \quad \mathbf{c}_l = c_l/c_s, \quad \mathbf{x} = \frac{x}{R}, \quad \mathbf{y} = \frac{y}{R},$$

$$\tau = \frac{k_s t}{R^2}, \quad \theta = \frac{T - T_m}{T_m - T_0}, \quad \mathbf{L} = \frac{1}{St}$$

where R is a characteristic length, and St is the Stefan number defined as:

$$St = \frac{c_s(T_m - T_0)}{L}.$$

4.2. *The direct problem*

The first example considered is that of a square 2×2 which is filled with liquid at the melting point ($\theta_i = 0$). The surface is suddenly cooled to $\theta_0 = -1$.

Figure 2 shows the interface locations at various dimensionless times τ. Figures 3 and 4 show interface progression with time along the adiabatic ($x_1 = 1$) and diagonal ($x_1 = x_2$). The BEM results are here compared in Fig. 3 with the implicit finite difference solution of Rao and Sastri (1984), the work of Lazaridis (1969), and also in Fig. 4 with the semi-analytical solution of Rathjen and Jiji (1971). These BEM solutions compare very well with the solutions from other numerical schemes as is seen in Figs 3 and 4. Temperature calculations for some internal points are shown in Fig. 5.

The following example involves a square of 2×2 with

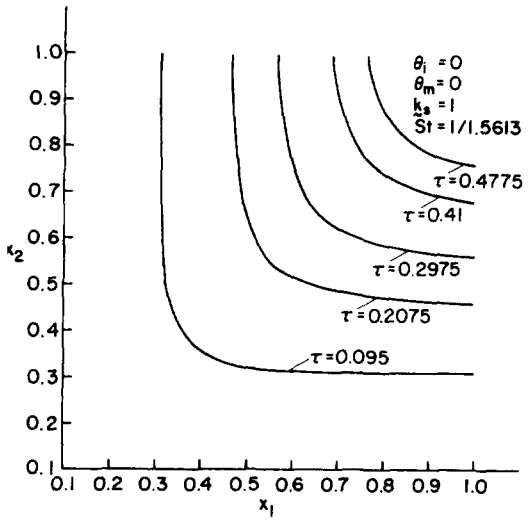

Fig. 2. Interface motion in a square mold as a function of time [from Zabaras and Mukherjee (1987)].

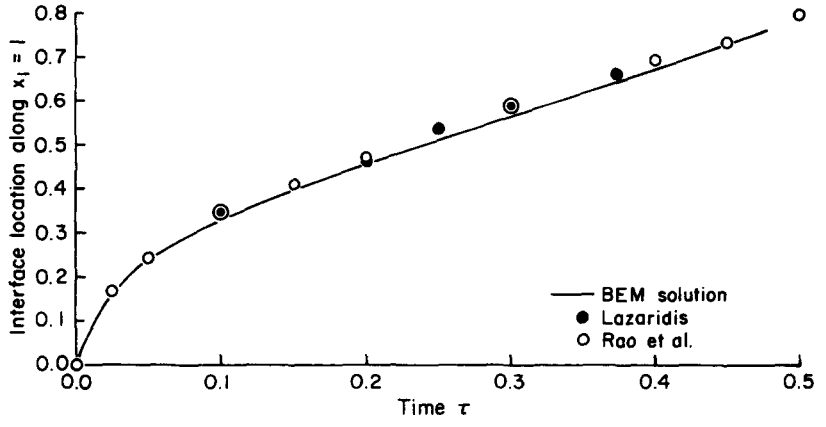

Fig. 3. Interface motion in a square mold along the adiabatic $x_1 = 1$ as a function of time. Same situation as in Fig. 2 [from Zabaras and Mukherjee (1987)].

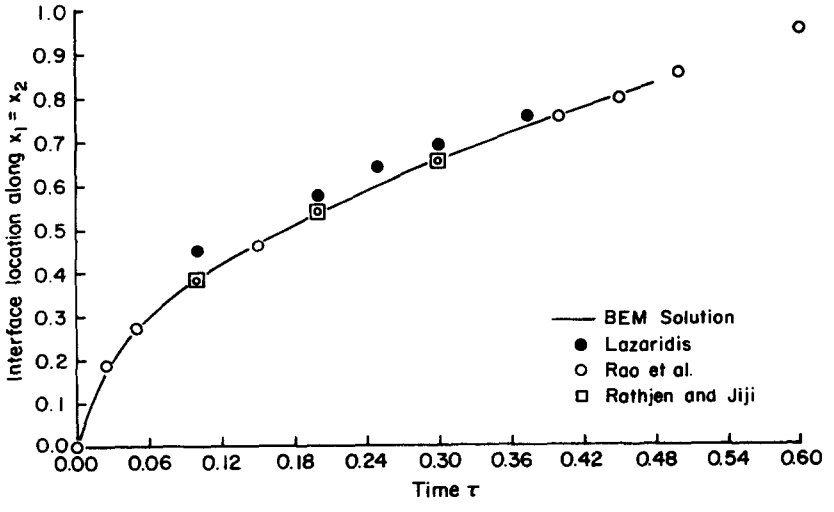

Fig. 4. Interface motion in a square mold along the diagonal $x_1 = x_2$ as a function of time. Same situation as in Fig. 2 [from Zabaras and Mukherjee (1987)].

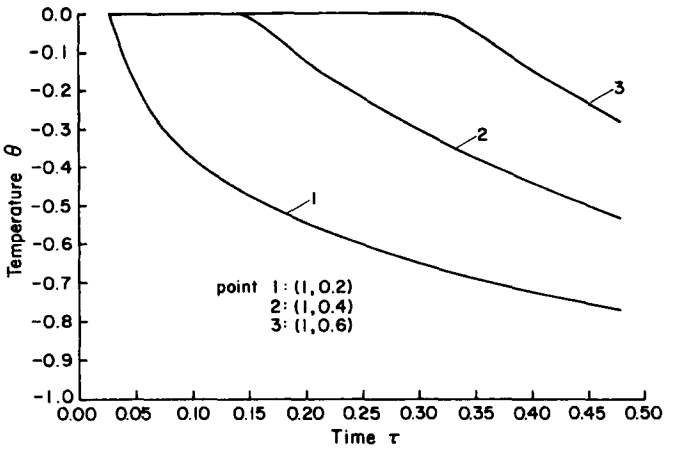

Fig. 5. Temperature distribution at some internal points with respect to time during solidification in a square mold. Same situation as in Fig. 2 [from Zabaras and Mukherjee (1987)].

$$\mathbf{c}_l = 1, \quad \mathbf{k}_l = 1, \quad \theta_0 = -1, \quad \theta_i = 0.3 \quad \text{and} \quad St = 4.$$

The same problem has been analysed previously by Budhia and Kreith (1973), Comini *et al.* (1974), Ralph and Bathe (1982) and Zabaras and Ruan (1990).

Figure 6 shows the front position on the diagonal ($x_1 = x_2$) and Fig. 7 the temperature at the internal point $x_1 = x_2 = 0.5$. In Fig. 6 comparison is made with Ralph and Bathe (1982). The time step for the BEM is $\Delta t = 0.0225$ and that for the FEM is $\Delta t = 0.02$. A similar comparison is made in Fig. 7 where two time steps have been used. The FEM results of Ralph and Bathe (1982) show a big difference with a change in time step from 0.02 to 0.1. They have been found not to be in good agreement with the semi-analytical solution of Rathjen and Jiji (1971) [see Zabaras and Ruan (1990)].

A similar example with

$$\mathbf{c}_l = 1, \quad k_l = 1, \quad \theta_0 = -1, \quad \theta_i = 1 \quad \text{and} \quad St = 2$$

has been analysed. Figure 8 shows the interface location at various times. Figures 9 and 10 compare the diagonal and asymptotic positions of the interface, respectively, with the results given by Rao and Sastri (1984). Figure 11 compares the temperature history at the center of the mold with Rao and Sastri (1984).

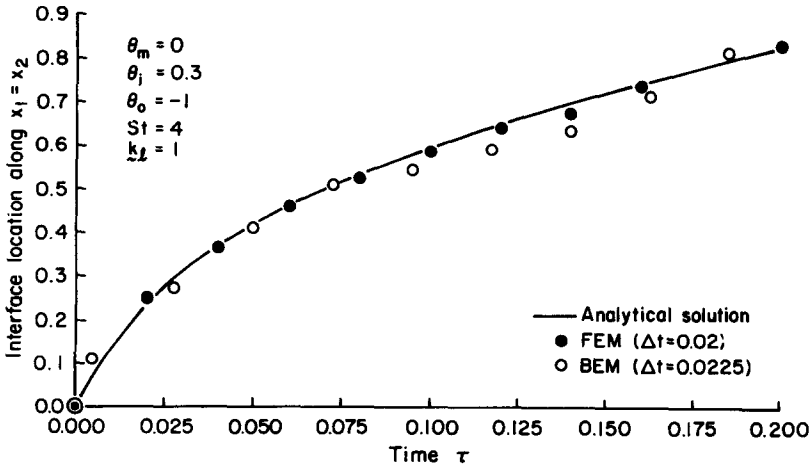

Fig. 6. Interface motion in a square mold along the diagonal $x_1 = x_2$ as a function of time. Analytical solution from Budhia and Kreith (1973). FEM solution from Ralph and Bathe (1982) [from Zabaras and Mukherjee (1987)].

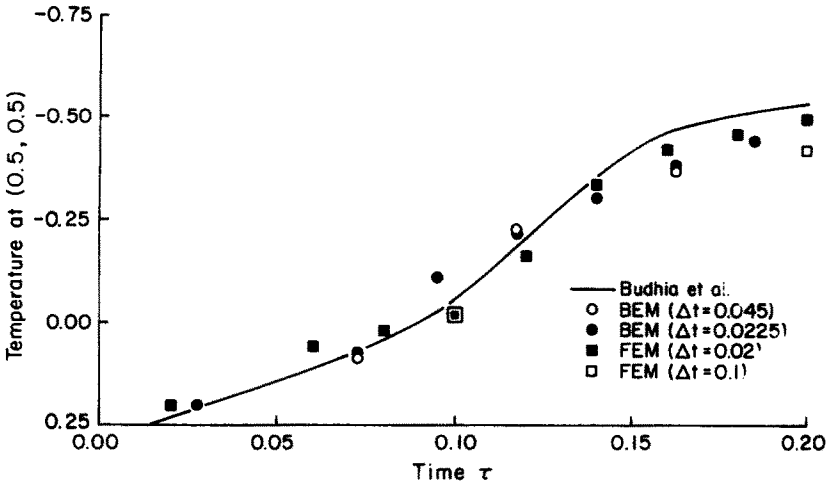

Fig. 7. Temperature history of the point (0.5, 0.5) during the solidification in a square mold. Same situation as in Fig. 6. FEM solution from Ralph and Bathe (1982) [from Zabaras and Mukherjee (1987)].

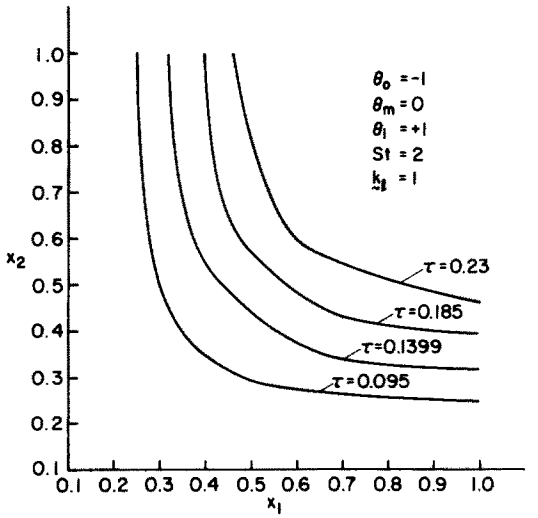

Fig. 8. Interface motion in a square mold as a function of time [from Zabaras and Mukherjee (1987)].

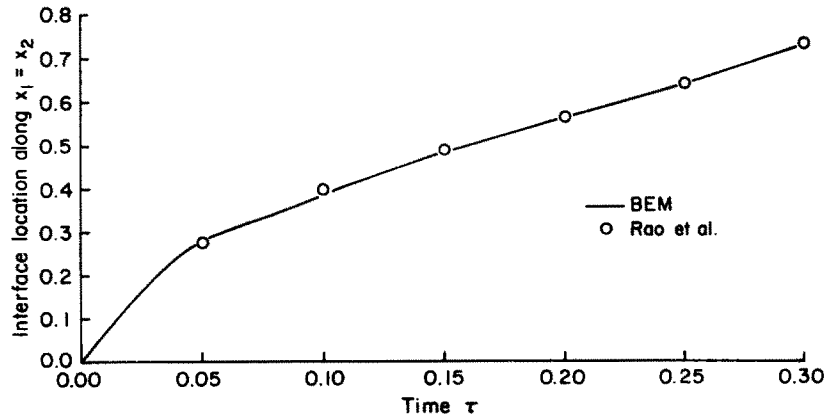

Fig. 9. Interface motion in a square mold along the diagonal $x_1 = x_2$ as a function of time. Same situation as in Fig. 8 [from Zabaras and Mukherjee (1987)].

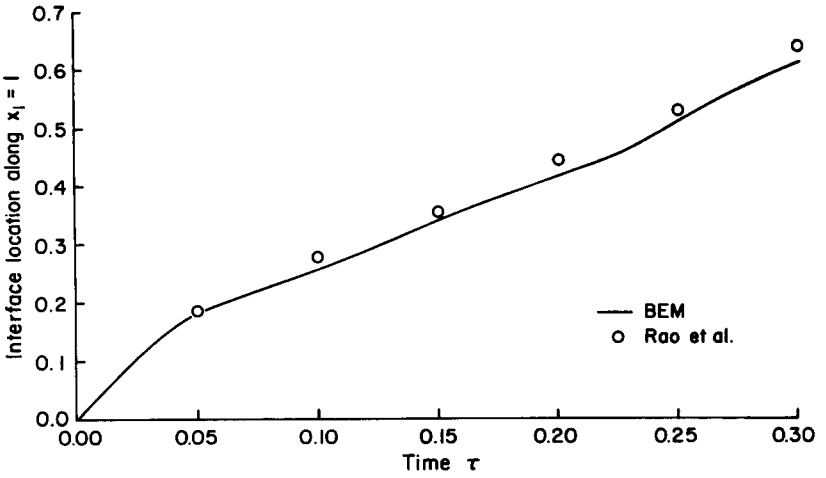

Fig. 10. Interface location in a square mold along the adiabatic ($x_1 = 1$) as a function of time. Same situation as in Fig. 8 [from Zabaras and Mukherjee (1987)].

In all the above examples the minimum time step was 0.0225 and the maximum 0.1. The error tolerance parameter $\varepsilon_{max} = 10^{-2}$. The equivalent heat capacity model has been used up to time 0.005 to initialize the BEM calculation. Double nodes have been considered both on ∂B_0 and ∂B_1.

4.3. *The design problem*

Consider solidification in a one-dimensional semi-infinite region $T_i = T_m = 0$, $K_s = 1$, $\rho_s = 1$, $c_s = 1$, $L = 1/2$ and $q_{ms} = 1$. Then $q_{ml} = 0$ and $V = 2$. The analytical solution of this problem is given as

$$q_{0s}(t) = e^{4t} \tag{35}$$

and

$$T_{0s}(t) = \tfrac{1}{2}(1-e^{4t}). \tag{36}$$

No spatial regularization is involved in this one-dimensional problem. The sensitivity

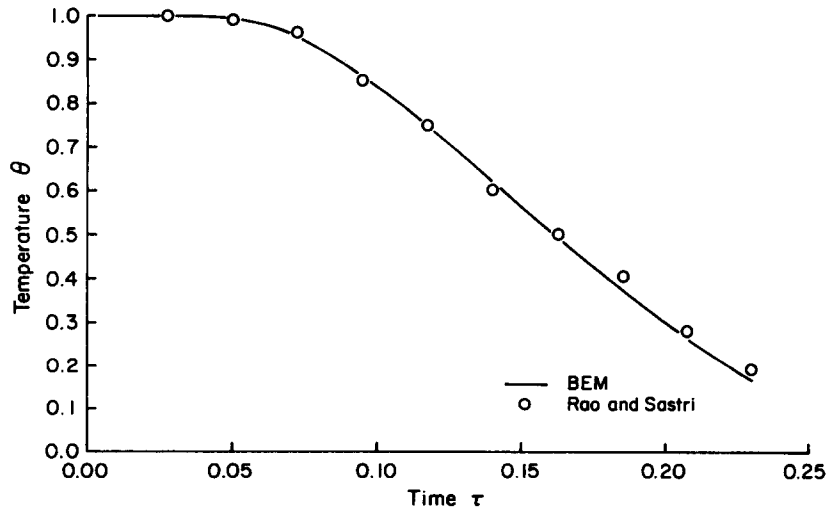

Fig. 11. Temperature distribution at the center of a square mold as a function at time. Same situation as in Fig. 8 [from Zabaras and Mukherjee (1987)].

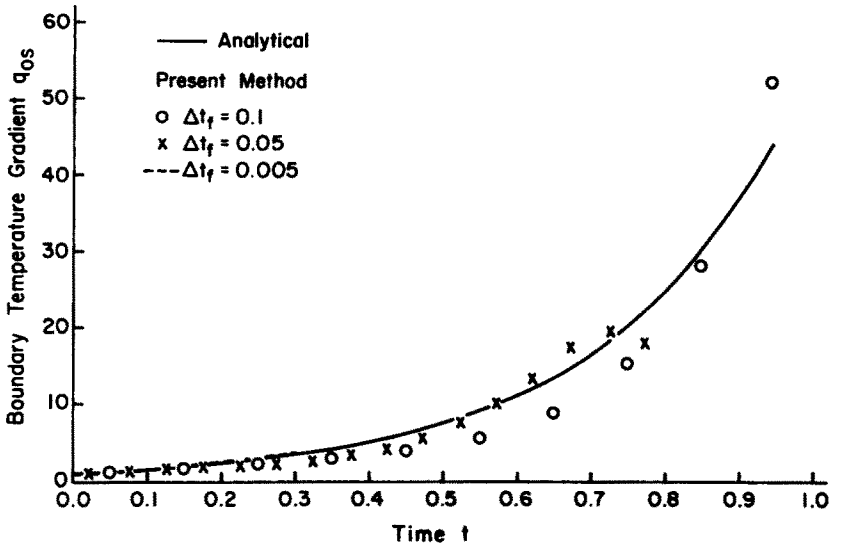

Fig. 12. Boundary temperature q_{0s} as a function of time for different time steps [from Zabaras *et al.* (1988)].

coefficients are calculated analytically in a way similar to that presented earlier. Figures 12 and 13 show plots of the flux $q_{0s}(t)$ together with the exact solutions given by eqns (35)–(36) for three different time steps, $\Delta t_f = 0.1$, 0.05 and 0.005. One future time step ($r = 2$) has been used to stabilize the solution. As expected, when the interface moves away from the $x = 0$ boundary, oscillations or divergence from the analytical solution occurs. In the above figures only the stable region has been plotted. As can be seen, the smaller the time step, the more accurate the numerical solution, but also the sooner it starts to diverge from the exact solution.

To test the algorithm in the liquid phase the following case is considered here:

$$T_i = -1, \quad T_m = 0, \quad k_l = 1, \quad K_l = 1, \quad \rho_l = 1, \quad c_l = 1,$$

$$L = 2, \quad l = 1, \quad V = \frac{0.43}{\sqrt{t}}, \quad h = 0.86\sqrt{t}, \quad q_{ml} = -0.76178\frac{1}{\sqrt{t}}.$$

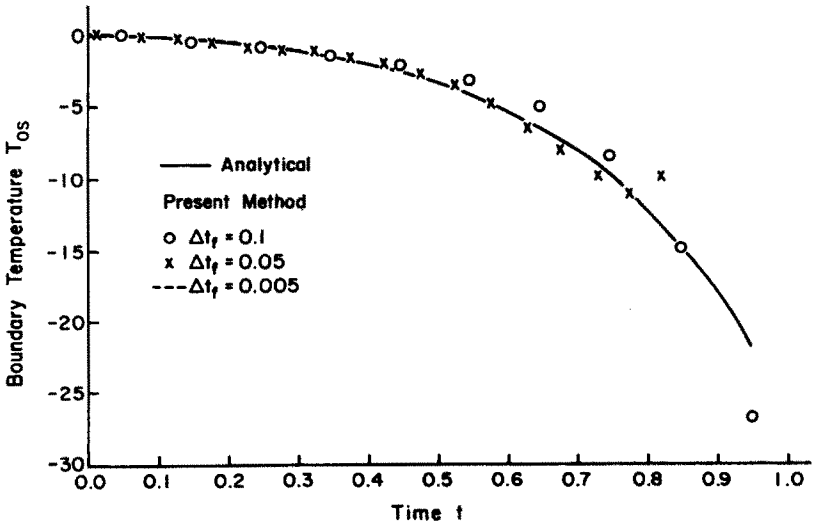

Fig. 13. Boundary temperature T_{0s} as a function of time for different time steps [from Zabaras *et al.* (1988)].

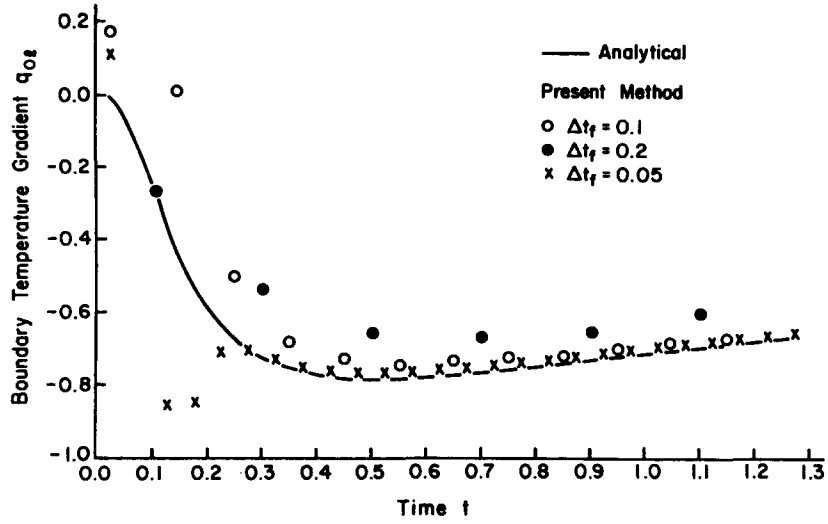

Fig. 14. Boundary temperature q_{0l} as a function of time for different time steps [from Zabaras *et al.* (1988)].

The above are approximations to the exact desired data that correspond to the following analytical solution:

$$q_{0l}(t) = 1.0437602\frac{1}{\sqrt{t}}e^{-1/4t}, \tag{37}$$

$$T_{0l}(t) = -1+1.850017 erfc\frac{1}{2\sqrt{t}} \tag{38}$$

[see Zabaras (1990)].

Figures 14 and 15 show the calculated temperature gradient and temperature at $x = l$. As expected the solution is inaccurate (still stable at early times), while very accurate and stable later. Note that if the exact desired data were used ($V = 0.432756/\sqrt{t}, q_{ms} = 0$) the estimated q_{0l} and T_{0l} are in very good agreement with the exact solutions (37) and (38).

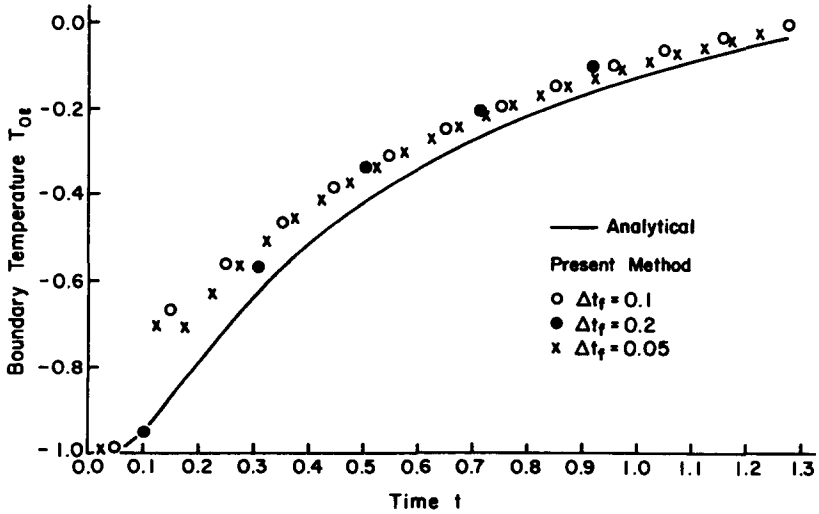

Fig. 15. Boundary temperature T_{0l} as a function of time for different time steps [from Zabaras *et al.* (1988)].

Acknowledgements—N.Z. acknowledges NSF support of his inverse solidification work under grant CBT-8802069 to the University of Minnesota and grant CTS-9115438 to Cornell University. S.M. acknowledges NSF grants numbers MSS8922185 and DMC-8421258 to Cornell University. The computing was supported by the Cornell National Supercomputing Facility.

REFERENCES

Albert, M. R. and O'Neill, K. (1986). Moving boundary–moving mesh analysis of phase change using finite elements with transfinite mappings. *Int. J. Numer. Meth. Engng* **23,** 591–607.

Banerjee, P. K. and Shaw, R. P. (1982). Boundary element formulation for melting and solidification problems. In *Developments in Boundary Element Methods* (Edited by P. K. Banerjee and R. P. Shaw), Vol. 2, pp. 1–18. Barking.

Beck, J. V., Blackwell, B. and St Clair, C. R. (1985). *Inverse Heat Conduction, Ill-posed Problems*. Wiley-InterScience, New York.

Bonnerot, R. and Janet, P. (1977). Numerical computation of the free boundary for the two-dimensional Stefan problem by space–time finite elements. *J. Comput. Phys.* **25,** 163–181.

Brebbia, C. A., Telles, J. C. and Wrobel, L. C. (1984). *Boundary Element Techniques—Theory and Applications in Engineering*. Springer, Berlin.

Budhia, H. and Kreith, F. (1973). Heat transfer with melting or freezing in a wedge. *Int. J. Heat Mass Transfer* **16,** 195–211.

Chuang, Y. K. and Szekely, J. (1972). On the use of Green's functions for solving melting and solidification problems. *Int. J. Heat Mass Transfer* **15,** 1171–1174.

Crank, J. (1984). *Free and Moving Boundary Problems*. Clarendon Press, Oxford.

Crank, J. and Gupta, R. (1975). Isotherm migration method in two dimensions. *Int. J. Heat Mass Transfer* **18,** 1101–1117.

Flemings, M. C. (1974). *Solidification Processing*. McGraw-Hill, New York.

Heinlein, M., Mukherjee, S. and Richmond, O. (1986). A boundary element method analysis of temperature fields and stresses during solidification. *Acta Mech.* **59,** 58–81.

Hong, C. P., Umeda, T. and Kimura, Y. (1984). Numerical models for casting solidification: Part II. Application of the boundary element method to solidification problems. *Metall. Trans. B* **15B,** 101–107.

Hsiao, J. S. (1985). An efficient algorithm for finite-difference analysis of heat transfer with melting and solidification. *Numer. Heat Transfer* **8,** 653–666.

Lazaridis, A. (1969). A numerical solution of the solidification (or melting) problem in multidimensional space. Doctoral dissertation, Columbia University.

Lynch, R. D. (1982). Unified approach to simulation on deforming elements with application to phase change problems. *J. Comput. Phys.* **47,** 387–411.

Murray, W. D. and Landis, F. (1959). Numerical and machine solutions of transient heat-conduction problems involving melting or freezing. *Trans. ASME(c), J. Heat Transfer* **81,** 106–112.

O'Neill, K. (1983). Boundary integral equation solution of moving boundary phase change problems. *Int. J. Numer. Meth. Engng* **19,** 1825–1850.

Ralph, W. and Bathe, K.-J. (1982). An efficient algorithm for analysis of nonlinear heat transfer with phase changes. *Int. J. Numer. Meth. Engng* **18,** 119–134.

Rao, P. and Sastri, V. M. K. (1984). Efficient numerical method for two-dimensional phase change problems. *Int. J. Heat Mass Transfer* **27**(11), 2077–2084.

Rathjen, K. A. and Jiji, L. M. (1971). Heat conduction with melting or freezing in a corner. *J. Heat Transfer, Trans. ASME* **93,** 101–109.

Roose, J. and Storrer, W. O. (1984). Modelization of phase changes by fictitious heat flow. *Int. J. Numer. Meth. Engng* **20,** 217–225.

Ruan, Y. and Zabaras, N. (1991). An inverse finite element technique to determine the change of phase interface location in two-dimensional melting problems. *Commun. Appl. Numer. Meth.* **7,** 325–338.

Sadegh, A., Jiji, L. M. and Weinbaum, S. (1985). Boundary integral equation technique with application to freezing around a buried pipe. ASME paper presented at the Winter Annual Meeting, Miami Beach, Florida, 17–21 November.

Tikhonov, A. N. and Arsenin, V. Y. (1977). *Solution of Ill-posed Problems*. V. H. Winston and Sons, Washington, DC.

Voller, V. R. and Cross, M. (1981). Accurate solutions of moving boundary problems using the enthalpy method. *Int. J. Heat Mass Transfer* **24,** 545–556.

Zabaras, N. (1990). Inverse finite element techniques for the analysis of solidification processes. *Int. J. Numer. Meth. Engng* **29,** 1569–1587.

Zabaras, N. and Mukherjee, S. (1987). An analysis of solidification problems by the boundary element method. *Int. J. Numer. Meth. Engng* **10,** 1879–1900.

Zabaras, N. and Ruan, Y. (1989). A deforming FEM analysis of inverse Stefan problems. *Int. J. Numer. Meth. Engng* **28,** 295–313.

Zabaras, N. and Ruan, Y. (1990). Moving and deforming finite element simulation of two-dimensional Stefan problems. *Comm. Appl. Numer. Meth.* **6,** 495–506.

Zabaras, N., Morellas, V. and Schnur, D. (1989). Spatially regularized solution of inverse elasticity problems using the boundary element method. *Comm. Appl. Numer. Meth.* **5,** 547–553.

Zabaras, N., Mukherjee, S. and Richmond, O. (1988). An analysis of inverse heat transfer problems with phase changes using an integral method. *J. Heat Transfer ASME* **110,** 554–561.

Zabaras, N., Ruan, Y. and Richmond, O. (1992). On the design of two-dimensional Stefan processes with desired freezing front motions. *Numer. Heat Transfer* **21B,** 307–325.